Nikon BioImaging Lab

Let us do the imaging for you.

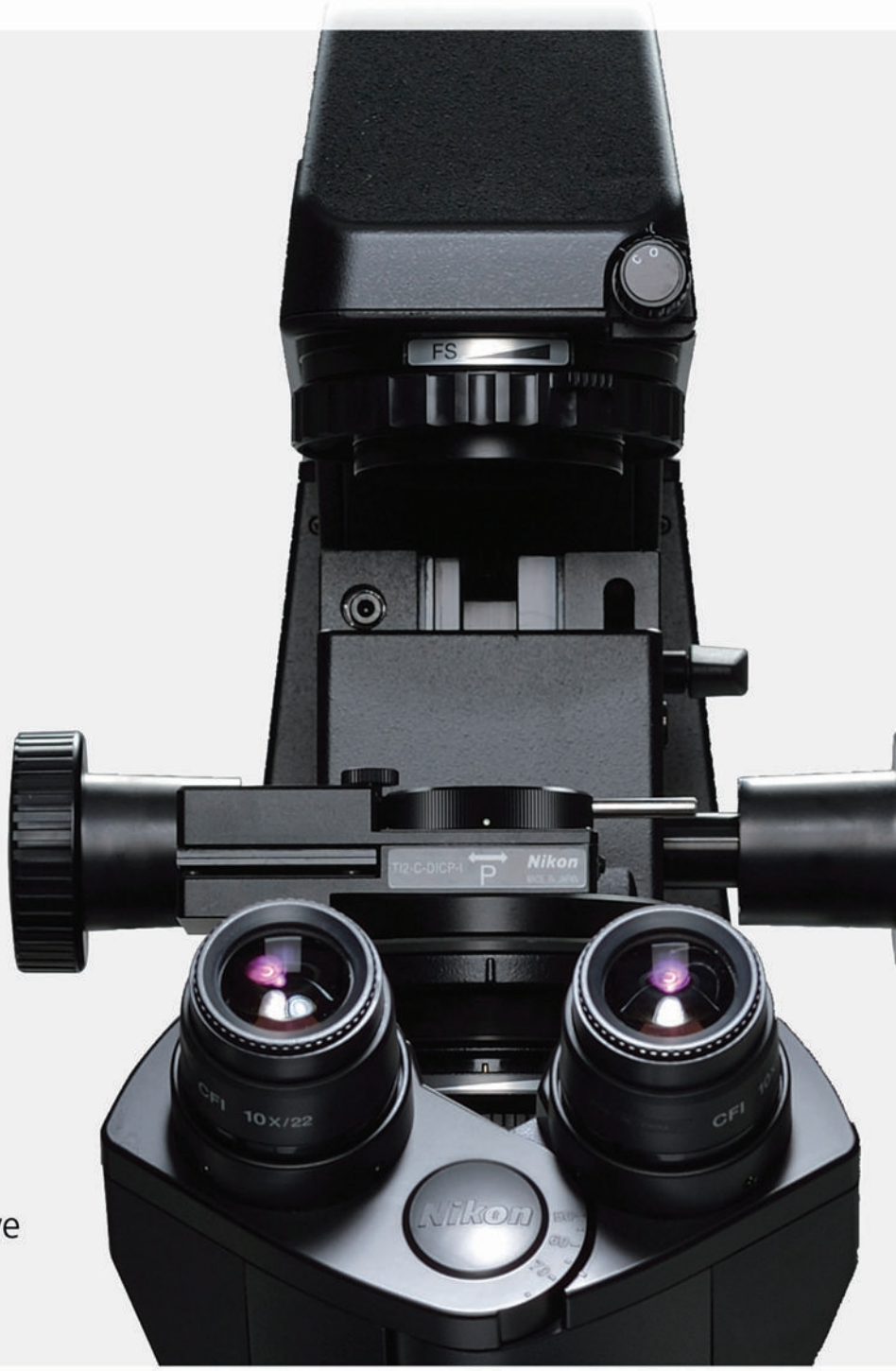

The Nikon BioImaging Lab is a state-of-the-art facility located in Cambridge, Massachusetts, that provides advanced technologies to support the burgeoning regenerative medicine and biotech sector.

For more information, visit www.microscope.healthcare.nikon.com/bioimaging-lab

Nikon Instruments Inc. ■ www.microscope.healthcare.nikon.com ■ nikoninstruments@nikon.net

STEM CELLS®

TISSUE-SPECIFIC STEM CELLS

Hematopoietic Stem Cell Dynamics Are Regulated by Progenitor Demand: Lessons from a Quantitative Modeling Approach

MARKUS KLOSE,[a] MARIA CAROLINA FLORIAN,[b,c] ALEXANDER GERBAULET,[d] HARTMUT GEIGER,[c,e] INGMAR GLAUCHE[a]

Key Words. Hematopoiesis • Hematopoietic stem cells • Regeneration • Aging • Mathematical modeling

[a]Institute for Medical Informatics and Biometry, Carl Gustav Carus Faculty of Medicine, Technische Universität Dresden, Dresden, Germany; [b]Center for Regenerative Medicine in Barcelona (CMRB), Bellvitge Biomedical Research Institute (IDIBELL), Hospital Duran i Reynals, Barcelona, Spain; [c]Institute of Molecular Medicine and Stem Cell Aging, University of Ulm, Ulm, Germany; [d]Institute for Immunology, Carl Gustav Carus Faculty of Medicine, Technische Universität Dresden, Dresden, Germany; [e]Division of Experimental Hematology and Cancer Biology, Cincinnati Children's Hospital Medical Center, University of Cincinnati, Cincinnati, Ohio, USA

Correspondence: Ingmar Glauche, Ph.D., Institute for Medical Informatics and Biometry, Carl Gustav Carus Faculty of Medicine, Technische Universität Dresden, Fetscherstr. 74, 01307 Dresden, Germany. Telephone: 49-0351-458-6060; e-mail: ingmar.glauche@tu-dresden.de

Received October 1, 2018; accepted for publication March 2, 2019; first published online March 21, 2019.

http://dx.doi.org/10.1002/stem.3005

ABSTRACT

The prevailing view on murine hematopoiesis and on hematopoietic stem cells (HSCs) in particular derives from experiments that are related to regeneration after irradiation and HSC transplantation. However, over the past years, different experimental techniques have been developed to investigate hematopoiesis under homeostatic conditions, thereby providing access to proliferation and differentiation rates of hematopoietic stem and progenitor cells in the unperturbed situation. Moreover, it has become clear that hematopoiesis undergoes distinct changes during aging with large effects on HSC abundance, lineage contribution, asymmetry of division, and self-renewal potential. However, it is currently not fully resolved how stem and progenitor cells interact to respond to varying demands and how this balance is altered by an aging-induced shift in HSC polarity. Aiming toward a conceptual understanding, we introduce a novel in silico model to investigate the dynamics of HSC response to varying demand. By introducing an internal feedback within a heterogeneous HSC population, the model is suited to consistently describe both hematopoietic homeostasis and regeneration, including the limited regulation of HSCs in the homeostatic situation. The model further explains the age-dependent increase in phenotypic HSCs as a consequence of the cells' inability to preserve divisional asymmetry. Our model suggests a dynamically regulated population of intrinsically asymmetrically dividing HSCs as suitable control mechanism that adheres with many qualitative and quantitative findings on hematopoietic recovery after stress and aging. The modeling approach thereby illustrates how a mathematical formalism can support both the conceptual and the quantitative understanding of regulatory principles in HSC biology. STEM CELLS *2019;37:948–957*

SIGNIFICANCE STATEMENT

Over the last decades, the average life expectancy of people in industrialized societies has considerably increased. It has become evident that healthy aging plays a crucial role for sustaining life quality among the elderly. However, many aging-related changes on both molecular and cellular levels are still undiscovered. This study investigates aging of the blood forming system, known as hematopoiesis. In particular, it focuses on blood stem cells that are able to reconstitute the entire blood system after injury. By investigating cellular mechanisms that are altered upon aging, the study reveals potential targets to be tackled for sustaining a healthy lifespan.

INTRODUCTION

Regenerating tissues contain stem cells as source for tissue replacement and repair. In the blood system, hematopoietic stem cells (HSCs) have been characterized as a rare cell population with usually slow turnover. The turnover can be dramatically accelerated in stress situations such as cytotoxic treatments or post-transplantation [1–4]. Most of the findings on the function of HSCs have been derived in conditions in which these cells were transplanted. In fact, regeneration of the hematopoietic system after cell transplantation into an irradiated host is still considered to be the gold standard for a functional definition of HSCs. Minimally invasive methods for marking of HSCs [5–15] recently allowed studying the hematopoietic system in unperturbed, that is, not transplanted, settings, thereby adding new insights into the functional role of HSCs and their progenitor populations. Based on these new findings, it appears that multipotent progenitors (MPPs) ensure the long-term supply with functional, differentiated hematopoietic cells in the homeostatic situation, while rarely depending on the

turnover of the HSC population. Most surprisingly, it has been shown that primitive HSCs rarely regenerate after targeted stem and progenitor cell depletion without extensive preconditioning [8]. The question remains how such a stable regenerating system needs to be regulated to appropriately respond to differentially changing demands.

Furthermore, there is increasing evidence that the population of HSCs itself is heterogeneous, with respect to both phenotype and functional potential [16]. Although transplantation studies have indicated a functional and heritable heterogeneity in the potential of HSC to differentiate into distinct lineages [17–19], the analysis of cell cycle activity by label retention studies [2, 20–24] revealed that more quiescent HSCs retain a higher repopulation capacity. Furthermore, microscopic studies discovered that more quiescent HSCs preferentially occupy distinct niches, whereas more proliferative cells appear closer to vascular structures [25–28]. These functional changes can also be identified on the phenotypic level, as refined phenotypic markers, such as Kit [29] or retinoic acid (RA) signaling [30, 31], allow for further subdivision of the HSC population.

In addition, it has also been shown that the hematopoietic system undergoes dramatic changes with age, most prominently characterized by an increasing contribution toward myeloid cell types at the expense of lymphoid differentiation, the overall loss of regenerative potential and an increase in the number of phenotypically defined, long-term repopulating HSCs (LT-HSCs) [32–44]. A single, causative reason for this aging phenotype has not been identified yet, although different mechanisms have been postulated such as accumulating DNA damage, increasing ROS levels, replication stress, loss of autophagy, or telomere shortening [33, 34, 37, 45–49]. Recently, it has become increasingly prominent that especially the declining integrity of epigenetic signatures in stem and progenitor cells might be directly involved in the functional deregulation of aged HSCs. The potential reasons for this epigenetic aging are manifold. Previous findings further identified a tight link between the regulation of cell polarity and distinct epigenetic marks [36, 50–52]. Most importantly, it could be shown that polarity was lost with age, thereby leading to more apolar cells that will undergo symmetric cell divisions [53]. The consequences of such a shift in the ability to undergo asymmetric cell divisions on the level of the population of HSCs is unknown.

Hematopoietic regeneration is usually depicted as a hierarchical process in which HSCs continuously contribute to a downstream, subsequently amplifying set of cell compartments. Experimental results on the role of HSC turnover in both the homeostatic and the challenged situation are essential to estimate the contribution of individual cell populations to the overall hematopoietic maintenance under changing demands as well as upon aging. Mathematical formalisms are essential to derive interpretable approximations of quantities that are not experimentally accessible yet, such as rates of HSC turnover [2, 6, 54] or the "flux" between cell populations. Moreover, beyond supporting the data analysis, mathematical models represent essential tools to translate biological hypotheses into quantitative and testable predictions. Such models are instrumental to speculate about functional mechanisms and to provide an unbiased and minimalistic view on the role of regulatory principles in hematopoiesis.

We aim to present a novel mathematical model of HSC organization that integrates HSC heterogeneity and aging-related changes in HSC divisional asymmetry, while explicitly accounting for the ambivalence between hematopoietic maintenance in the unchallenged homeostatic situation and immediate stress response. We mimic the intrinsic HSC heterogeneity by assuming a separation between repopulating HSCs (rpHSCs), which are rarely activated during homeostasis and preferentially divide asymmetrically, and maintaining HSCs (mtHSCs), which ensure the continuous supply of progenitor cells for downstream hematopoiesis. Our model establishes a unifying framework which reproduces both the rare contribution [6] and the slow recovery of HSCs in the homeostatic situation [6, 8, 9, 55], as well as the accelerated responses after perturbation (see references in [4]). The model extends to address the apparent increase in phenotypic HSCs as a consequence of an impaired HSC control due to the loss of cell polarity and the consequent inability of the cells to divide asymmetrically [53]. Our model suggests a dynamically regulated population of intrinsically asymmetrically dividing HSCs as suitable control mechanism that adheres with many qualitative and quantitative findings on hematopoietic recovery after stress and aging.

Materials and Methods

Model Setup

We present a simple mathematical model based on ordinary differential equations (ODEs) describing proliferation and differentiation of rpHSC, mtHSC, and progenitor populations (Fig. 1A). The model has the following features:

- **Turnover and repopulation.** All cells are able to proliferate with respective rates p and differentiate into downstream compartments. We do not explicitly account for apoptotic events, but interpret proliferation rates as a net effect. Additionally, the effective proliferation of rpHSCs $p_{\mathrm{rp,\ eff}}$ is regulated according to the *demand* within the mtHSC compartment. Technically, this is implemented as a logistic growth limitation, where $p_{\mathrm{rp,eff}}(t) = p_{\mathrm{rp,max}}\left(1-\frac{N_{\mathrm{mt}}(t)}{K}\right)$ with a carrying capacity K.

- **Symmetry of rpHSC division.** For rpHSCs, we consider symmetric divisions (with rate s, ranging between 0 and 1), in which both daughter cells retain the rpHSC identity, and asymmetric divisions (with rate $1-s$), in which one daughter remains a stem cell, whereas the other daughter cell instantly differentiates into the downstream mtHSC compartment. We neglect the possibility of symmetric divisions with both daughters immediately differentiating. To account for division-independent differentiation of rpHSCs, we introduce a parameter d_0 describing a simple additional flux from the rpHSC to the mtHSC compartment.

- **Aging.** We account for an age-dependent change of the fraction of symmetric cell divisions by explicitly formulating the symmetry parameter $s = s(t)$ as a time-dependent quantity.

The resulting ODE describes the dynamics of the rpHSC compartment in terms of cell numbers $N_{\mathrm{rp}}(t)$:

$$\dot{N}_{\mathrm{rp}}(t) = s \cdot p_{\mathrm{rp,max}}\left(1-\frac{N_{\mathrm{mt}}(t)}{K}\right)N_{\mathrm{rp}}(t) - d_0 N_{\mathrm{rp}}(t).$$

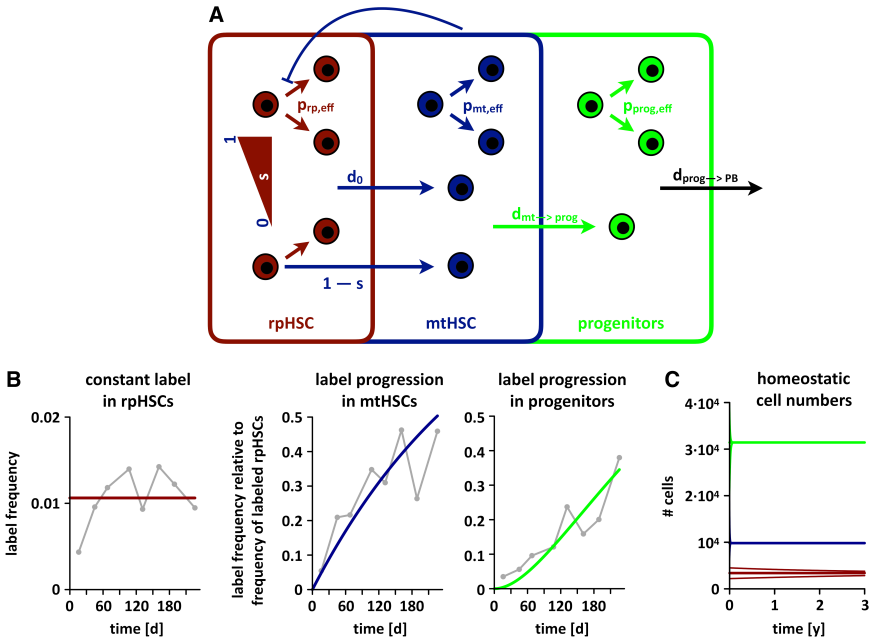

Figure 1. Model setup and parameter estimation. **(A):** Sketch of the mathematical model setup. Repopulating hematopoietic stem cells (rpHSCs; red) are able to proliferate with an effective proliferation rate $p_{rp,\ eff}$ which is regulated by maintaining HSC (mtHSC) demand. rpHSCs differentiate instantly after division according to symmetry parameter $0 < s < 1$. Additionally, the model incorporates a background differentiation of d_0. mtHSCs (blue) and progenitors (green) are able to proliferate and differentiate with respective rates p and d. Additionally, there is an influx from the respective upstream compartment. **(B):** Label progression time courses for the homeostatic parameter set in Table 1 for rpHSCs (red), mtHSCs (blue), and progenitors (green), respectively. Gray curves correspond to label progression data by [6] for long-term HSC, short-term HSC, and MPP compartments. **(C):** Depiction of the model's unique steady state solution (color coding as in [A]). Thick lines depict homeostatic cell numbers (i.e., the analytic steady state) for the estimated parameter set shown in Table 1. Thin lines represent time courses for arbitrary initial cell numbers. Initial values have been varied separately for each cell type, while leaving the other cell numbers at their respective steady state value.

Consequently, the subsequent downstream compartment, namely mtHSCs, is described as follows:

$$\dot{N}_{mt}(t) = (1-s)\cdot p_{rp,\,max}\left(1-\frac{N_{mt}(t)}{K}\right)N_{rp}(t) + d_0 N_{rp}(t) + p_{mt,\,max}\left(1-\frac{N_{mt}(t)}{K_{mt}}\right)N_{mt}(t) - d_{mt\to prog}N_{mt}(t).$$

Herein, $(1 - s)$ refers to the proportion of rpHSCs which differentiate due to asymmetric cell division, whereas the influx of cells due to background differentiation of rpHSCs is described by $d_0 N_{rp}(t)$. mtHSCs proliferate with an effective rate $p_{mt,\,max}\left(1-\frac{N_{mt}(t)}{K_{mt}}\right)$ and differentiate with rate $d_{mt\,\to\,prog}$.

Furthermore, in the progenitor compartment, cells proliferate with an effective rate $p_{prog,\,max}\left(1-\frac{N_{prog}(t)}{K_{prog}}\right)$ and differentiate with rate $d_{prog\,\to\,PB}$ to further downstream compartments. $d_{mt\,\to\,prog}N_{mt}(t)$ denotes the influx from the mtHSC to the progenitor compartment. The resulting ODE for the progenitor compartment reads:

$$\dot{N}_{prog}(t) = d_{mt\to prog}N_{mt}(t) + p_{prog,\,max}\left(1-\frac{N_{prog}(t)}{K_{prog}}\right)N_{prog}(t) - d_{prog\to PB}N_{prog}(t).$$

Furthermore, downstream compartments can be integrated by sequentially adding compartments as proposed in [6].

Parameter Estimation

In order to identify an optimal parameterization of the mathematical model based on available data sets, we postulate that the topmost rpHSCs share many features (such as pronounced quiescence and high repopulation behavior) with phenotypically defined LT-HSCs, whereas mtHSCs are more similar to short-term HSCs (ST-HSCs). Furthermore, we map the progenitor compartment to MPPs. In order to estimate cell turnover and differentiation, we use label progression data in a homeostatic system from [6], in which the Tie2+ HSC population has been identified as the subset with the highest reconstitution potential [56], thereby matching our concept of rpHSCs. This approach enables us to apply a maximum likelihood method which minimizes the residual sum of squares between the model simulation and available data. To appropriately account for this data type, we split each compartment in a labeled and an unlabeled fraction obeying the same parameters (see Supporting Information for further details of the mathematical approach).

Since label progression data was acquired in young mice, we assume that approximately 80% of LT-HSC divisions are asymmetric [53], thereby fixing the symmetry parameter $s = 0.2$ accordingly. Moreover, we adhere to estimates from [6] reporting that MPPs differentiate with rate $d_{MPP\,\to\,CMP} = 3.992$ per day to the common myeloid progenitor (CMP) compartment and with rate $d_{MPP\,\to\,CLP} = 0.022$ per day to the common lymphoid progenitor (CLP) compartment, yielding a total progenitor outflux of $d_{prog\,\to\,PB} = 4.014$ per day. As an upper limit for rpHSC turnover, we fix $p_{rp,\ max} = 0.5$ per day. Due to the logistic growth limitation,

Table 1. Table of fitted values for estimated (upper part) and assigned (lower part) parameter values in a homeostatic system

Parameter	Fitted value	Biological interpretation
d_0	0.002 per day	Background differentiation rate of rpHSCs
$p_{mt,\ eff}$	0.033 per day	Effective proliferation rate of mtHSCs
$d_{mt \rightarrow prog}$	0.036 per day	Differentiation rate of mtHSCs
$p_{prog,\ eff}$	4.003 per day	Effective proliferation rate of progenitors
$p_{rp,\ max}$	0.5 per day	Maximum proliferation rate of rpHSCs
s	0.2	Proportion of symmetric rpHSC divisions
K	10,000 cells	Carrying capacity for demand regulation of rpHSCs
$d_{prog \rightarrow PB}$	4.014 per day	Differentiation rate of progenitors

Abbreviations: rpHSCs, repopulating HSCs; mtHSCs, maintaining HSCs.

this value is achieved only in the limiting case of an empty mtHSC compartment and does not qualitatively influence our findings in steady state. We further make use of steady state compartment size ratios as estimated in [6], where $\frac{N_{mt}}{N_{rp}} = \frac{N_{ST}}{N_{LT}} = 2.9$ and $\frac{N_{prog}}{N_{mt}} = \frac{N_{MPP}}{N_{ST}} = \frac{9}{2.9}$. In our model formulation, these steady state compartment size ratios are independent from the carrying capacity K (see Supporting Information for further mathematical details). Therefore, we arbitrarily set K = 10,000. Moreover, this allows us to reduce the set of parameters to be estimated to the rpHSC background differentiation rate d_0 and the effective proliferation rate of progenitors $p_{prog,\ eff}$ in steady state. Note that we only estimate a steady state value for the effective proliferation rate of progenitors here, since the label progression data was acquired in a homeostatic situation and therefore does not allow assessment of neither the maximum proliferation rate of progenitors $p_{prog,\ max}$ nor the respective carrying capacity K_{prog}. However, given a value for $p_{prog,\ max}$ and steady state values for $p_{prog,\ eff}$ and N_{prog}, a corresponding K_{prog} can be calculated explicitly (the same applies to the respective parameters of mtHSCs, see Supporting Information for further details).

Table 1 summarizes both assigned and estimated parameter values.

Results

Formulation of a Demand-Driven HSC Model

We study control mechanisms for the regulation of a heterogeneous HSC compartment. Within a mathematical modeling approach, we assume for the most primitive HSC subset, which we refer to as rpHSCs, that (i) the turnover of and the outflux from this population is demand-driven and regulated at the downstream level and that (ii) rpHSCs divide asymmetrically, whereas this ability declines with age. As a second and subsequent HSC subset, mtHSCs gain influx from rpHSCs, similar to the succeeding progenitors which for their part gain influx from upstream mtHSCs. Both mtHSCs and progenitors further differentiate and retain the ability to regulate their proliferation in order to ensure fast recovery after depletion. Technically, the model is implemented as a set of three sequentially aligned compartments representing populations of rpHSCs, mtHSCs, and progenitors (Fig. 1A, details in Materials and Methods). Assumption (i) is integrated as a logistic growth limitation of the rpHSC compartment, which is not regulated by the abundance of rpHSCs but by the saturation of the downstream mtHSCs. In homeostasis, this leads to a slow rpHSC turnover as well as a low contribution to the subsequent compartments, while in perturbation scenarios, both rpHSC turnover and differentiation are increased. The ability to undergo asymmetric cell division is incorporated as an explicit feature of rpHSCs. Hence, the deregulation of asymmetric rpHSC divisions with age (assumption [ii]) is modeled as an increase in the fraction of rpHSCs that divide symmetrically rather than asymmetrically. The system can be tuned to achieve configurations in which all three cell populations are present and stably contribute over time.

Applying the Model to Steady State Hematopoiesis

In order to obtain a model configuration that applies to murine hematopoiesis, we fit our model to quantitative data on label progression in the homeostatic situation. In a reference experiment, Busch et al. in vivo marked a small number of phenotypically defined LT-HSCs by using a YFP marker being almost uniquely inducible in LT-HSCs [6]. Assessment of the temporal abundance of marked cells in the downstream compartments allowed to interrogate cell turnover and fluxes. By identifying rpHSCs, mtHSCs and progenitors from our model with phenotypically defined LT-HSC, ST-HSC, and MPP populations [6], we are able to use this label progression data to estimate parameter values of our model. Unlike the mathematical model in [6], which does not account for a regulated rpHSC compartment, we here use this data to estimate parameters, such as proliferation and differentiation rates, of an advanced model that explicitly considers a regulation on the rpHSC level. By using an optimization routine, we obtain values for all model parameters which are provided in Table 1. Figure 1B illustrates that the parameterized model successfully describes the homeostatic situation in which the label slowly progresses from rpHSCs to mtHSCs and progenitors. We estimate that rpHSCs divide rarely, on average once per 111 days $\left(= \left[p_{rp,\ max} \cdot \left(1 - \frac{\tilde{N}_{mt}}{K} \right) \right]^{-1} \right)$. Similarly, background differentiation of rpHSCs is a very rare event in homeostasis with an estimated value of once per 557 days ($= d_0^{-1}$). In contrast, both mtHSCs and progenitors proliferate almost as fast as they differentiate.

Modeling Hematopoietic Stress Response

Unlike the homeostatic situation, hematopoietic recovery is mainly driven by HSCs, which are activated in response to stress. Accordingly, depletion of downstream blood cells pushes HSCs into cycle thereby increasing their differentiation and replenishing the system. Myeloablation is commonly initiated by cytotoxic drugs or ionizing radiation followed by transplantation of donor cells whose contribution to hematopoiesis is subsequently measured [2, 4, 57–59]. However, the preconditioning does not only impact on hematopoietic cells but also affects other hematopoietic niche cells of nonhematopoietic origin and thereby initiates further, indirect feedback loops that may influence hematopoietic recovery. Interestingly, Schoedel et al. established a perturbation model in which hematopoietic stem and progenitor cells were depleted in situ while minimizing the impact on other cell types [8]. They could show that upon multicompartment depletion, both ST-HSC and MPP populations quickly expanded close to steady state levels after few weeks only, whereas the LT-HSC compartment remained depleted for extended time periods.

In order to address the impact of different perturbations within our model system, we first considered three scenarios that only affect cell numbers: (a) multicompartment depletion, (b) downstream (i.e., both mtHSC and progenitor) depletion, and (c) rpHSC depletion. We mimicked those scenarios by

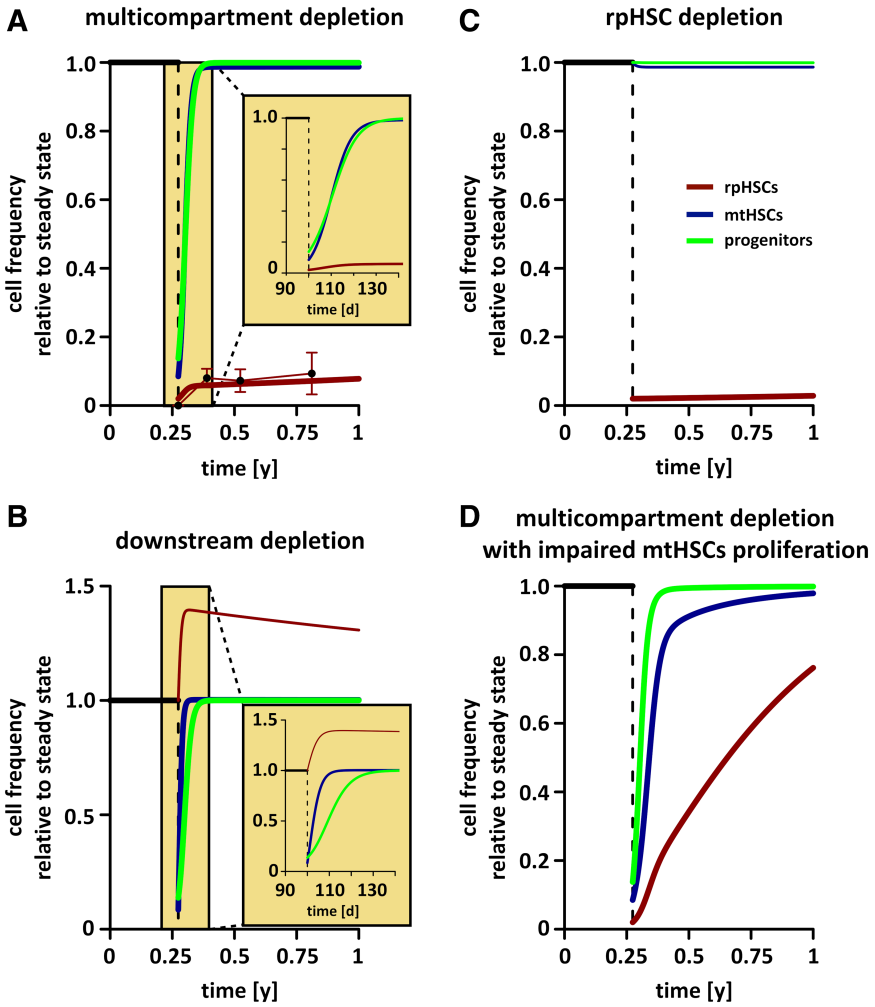

Figure 2. Hematopoietic stress response in a young mouse. Time courses, given in cell frequency relative to steady state cell numbers, illustrate the dynamic system response to targeted depletion (dashed vertical line at t = 0.25y) of selected cell stages. **(A):** Recovery of the system after almost complete depletion. Data points show long-term hematopoietic stem cell frequencies and the respective standard errors as presented in [8]. Inset depicts a detailed view on the recovery of the system with time being given in units of days. **(B):** Recovery after both maintaining HSC (mtHSC) and progenitor depletion. Inset allows a detailed view in time units of days. **(C):** Recovery after sole repopulating HSC depletion. **(D):** Recovery after almost complete depletion with impaired maximum mtHSC proliferation after irradiation ($p_{mt,\ max}$ = 0.1 per day) and gradual recovery. Time is given in units of years. The color scheme corresponds to the legend in (C). At time point zero, homeostatic cell numbers equal the steady state cell numbers obtained from Figure 1C. Thin lines represent the time course of unperturbed compartments. The aging-related loss of asymmetric division ability is neglected here, since it is not clear how this is affected upon cell loss.

reducing the initial values for mtHSCs and progenitors to the proportions measured in [8] for ST-HSC and MPP populations (Fig. 2A, 2C), while we fixed the level of rpHSCs to 2% of the homeostatic value.

In the case of multicompartment depletion (i.e., depletion of rpHSCs, mtHSCs, and progenitors, which is comparable to the experiments conducted by Schoedel et al.) our model predicts a fast recovery of progenitors and mtHSCs (Fig. 2A) to provide a sufficient supply of cells to peripheral blood. Here, the respective logistic growth limitations for both the mtHSC and progenitor compartments ensure a sufficiently fast recovery after depletion: Due to enhanced proliferation, both mtHSCs and progenitors regain their steady state levels within 1 month. Interestingly, the model predicts that the regeneration of the rpHSC pool is characterized by two phases (Fig. 2A): first, the rpHSCs, which have remained after depletion, are forced into cycle due to mtHSC demand resulting in an increase in cell numbers within the first days after depletion. When mtHSCs have reached their steady state value, rpHSC recovery slows down and cell numbers remain low. By identifying rpHSCs with phenotypic LT-HSCs, the model recapitulates the overall dynamic pattern observed for LT-HSC frequency data after depletion (Fig. 2A, data points) as reported in [8].

Upon downstream (both mtHSC and progenitor) depletion, both mtHSC and progenitor populations are predicted to recover after 10–20 days, as a consequence of their self-regulated proliferation (Fig. 2B). However, rpHSC proliferation is also rapidly enhanced thereby satisfying the demand of the mtHSC compartment. After this initial fast and strong increase, rpHSC numbers only slowly return back to steady state levels, possibly due to low background differentiation.

In contrast to the fast recovery of hematopoietic stem and progenitor compartments after downstream depletion, the model

predicts no return to the homeostatic situation, if only rpHSCs are targeted. In fact, it is the almost stable and ongoing turnover and differentiation of mtHSCs which does not pass on an increased demand to rpHSCs. Therefore, the population of rpHSCs experiences no recovery (Fig. 2C).

Hematopoietic cell depletion without affecting other cell types, for example, niche cells, is a comparably new technique to address hematopoietic stress response. More commonly, hematopoietic stress is induced by irradiation or cytotoxic treatments, thereby also impacting on the bone marrow microenvironment and reducing its supportive function. Consequently, we model multicompartmental cell depletion by irradiation as a reduction in cell numbers plus an impaired proliferation of mtHSCs. Technically, we decrease their maximum proliferation rate to $p_{mt,\ max} = 0.1$ per day after irradiation and let it gradually recover (see Supporting Information).

In this case of multicompartment depletion with impaired mtHSC proliferation, the model still predicts a fast recovery of progenitor cells due to their preserved self-regulated proliferation (Fig. 2D). In contrast, mtHSC recovery is delayed due to missing microenvironmental support modeled as a reduced proliferative ability. This leads to an increasing demand for rpHSCs to differentiate to the mtHSC compartment. As a consequence, rpHSCs are activated into cycle, leading to a pronounced increase in rpHSC numbers in the first weeks after stress induction. When mtHSC numbers have recovered, rpHSC proliferation slows down. However, since the recovery of the maximum proliferation rate of mtHSCs takes longer, there is still a demand for differentiating rpHSCs, resulting in an ongoing increase in rpHSC numbers due to an enhanced rpHSC proliferation.

In conclusion, our results indicate that the presented model successfully extends from the homeostatic situation to a qualitative and quantitative description of four reference scenarios associated with hematopoiesis under stress and regeneration. Our model extends these findings to the hypothesis that a differential regulation of HSC subsets is causative for the differences in the kinetics of HSC and progenitor recovery after stress induction.

Modeling Hematopoietic Aging

Several studies reveal that the abundance of phenotypic HSCs increases with age, while the functional potential of these cells declines [32–36, 40, 41]. However, the reasons for the pronounced increase in HSC number with aging are still not fully understood. It could be speculated that the low, albeit constant, demand of progenitor cells can only be met by a growing HSC pool that compensates for their declining functionality. In this context, we recently discussed the limited ability of aged HSCs to divide asymmetrically as a potential reason for their continuously increasing abundance [53]. In fact, we observed approximately 80% asymmetric divisions in HSCs derived from young mice, whereas this number declines to approximately 20% for aged donors. We raise the question whether this shift in the potential for asymmetric divisions is sufficient to explain the apparent increase in HSCs.

For a quantitative assessment, we measured cell frequencies of different HSC populations referred to as LT-HSC (gated as $Lin^{neg}c\text{-}kit^{+}sca\text{-}1^{+}CD34^{-/low}Flk2^{-}$), ST-HSC (gated as $Lin^{neg}c\text{-}kit^{+}sca\text{-}1^{+}CD34^{+}Flk2^{-}$) and LMPP (gated as $Lin^{neg}c\text{-}kit^{+}sca\text{-}1^{+}CD34^{+}Flk2^{+}$) populations in young (10–16 weeks old), middle-aged (40–54 weeks old), and old (more than 86 weeks old) C57BL/6 mice (Fig. 3A, see also Experimental Methods in Supporting Information). LT-HSC frequencies increase almost exponentially, while ST-HSC and MPP frequencies remain rather constant or, in the case of MPPs, even tend to decrease over the mouse lifespan. For a comparison of the data with our model, we considered compartment size ratios which describe the compartment size relative to the abundance of LT-HSCs. We found that the ST-HSC to LT-HSC ratio rapidly decreases within the first year and afterward remains constant, whereas the MPP to ST-HSC ratio slowly decreases with age (Fig. 3B). Since we assessed different marker combinations as compared with [6] to analyze the HSC populations, we obtained different compartment size ratios (see Experimental Methods in Supporting Information for further details).

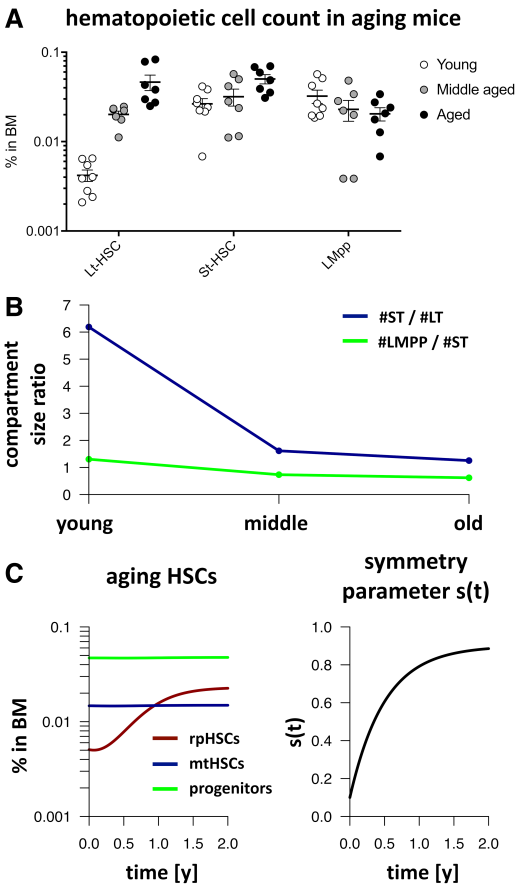

Figure 3. Hematopoietic aging. **(A):** Measured cell frequencies in long-term hematopoietic stem cell (HSC), short-term HSC, and LMPP compartments for young (10–12 weeks), middle-aged (40–54 weeks), and old (more than 86 weeks) mice. Vertical lines represent the standard error of the mean of the measurements (see Supporting Information for further details on cell sorting). **(B):** Measured compartment size ratios. **(C):** Cell frequencies predicted by the model (left-hand side) for a given changing $s(t)$ of the frequency of symmetric repopulating HSC divisions with age (right-hand side, see Supporting Information for further mathematical details). Cell frequencies are calculated by dividing the model solution by the median total BM cell number which was used for cell sorting.

In our modeling approach, we implemented a corresponding aging scenario by assuming that the rate of symmetric cell divisions in rpHSCs $s = s(t)$ increases from 10% in a "young system" to 90% in an "old system." Since the available data suggest a faster decrease in rpHSC to mtHSC ratio in the first compared

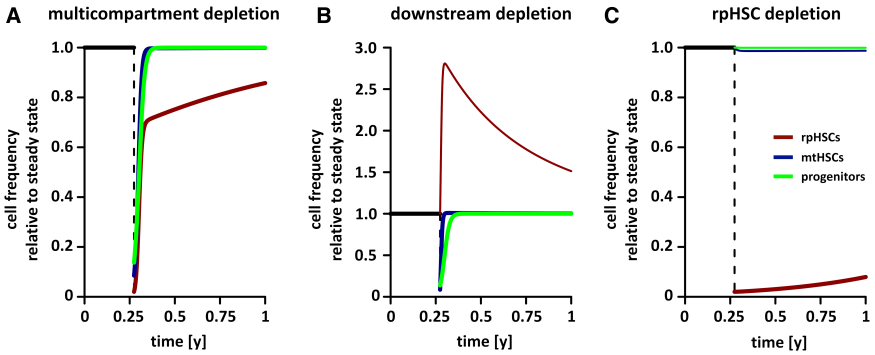

Figure 4. Hematopoietic stress response in an old mouse. Time courses, given in cell frequency relative to steady state cell numbers, illustrate the dynamic system response to targeted depletion (dashed vertical line at $t = 0.25y$) of selected cell stages. **(A):** Recovery of the system after almost complete depletion. **(B):** Recovery after both mtHSC and progenitor depletion. **(C):** Recovery after sole rpHSC depletion. Time is given in units of years. The color scheme corresponds to the legend in (C). At time point zero, homeostatic cell numbers equal the steady state cell numbers for the symmetry parameter $s = 0.8$. Thin lines represent the time course of unperturbed compartments.

with the second year, we chose a limited growth function for $s(t)$, which increases rapidly within the first year and saturates within the second year (Fig. 3C, see Supporting Information for mathematical details). By making these particular assumptions, we indeed see that the predicted frequency of rpHSCs in BM strongly increases similar to the biological observations, whereas the frequencies of mtHSCs and progenitors in BM remain rather constant (Fig. 3C). These findings illustrate that the increase in rpHSC frequency may derive from a compensatory mechanism, as with aging fewer rpHSCs with asymmetric division contribute to the downstream mtHSC compartment. The higher fraction of symmetric divisions expands the rpHSC pool, but does not affect the outflux, which is only regulated by mtHSC saturation level. Consequently, the model shows that there is no distinct change in the number of downstream cells. This confirms our experimental data and supports the prevailing notion that hematopoiesis in aged mice is still functional and does not suffer from severe insufficiencies in blood production.

To further use the capabilities of our modeling approach, we asked how a challenged hematopoietic system of an old mouse would recover after performing similar perturbation experiments as shown in the previous section, that is, (a) multicompartment depletion, (b) downstream (i.e., both mtHSC and progenitor) depletion, and (c) rpHSC depletion. Here, we defined an "old" mouse by assuming that the rate of symmetric rpHSC divisions s equals 0.8 whereas all other parameters remain unchanged. Thus, steady state rpHSC numbers are increased compared with a young mouse.

In the case of multicompartment depletion, the model predicts a fast increase of rpHSC numbers due to an interaction of enhanced proliferation driven by mtHSC demand and predominantly symmetric rpHSC division (Fig. 4A). As soon as mtHSC numbers get back to steady state levels, rpHSC proliferation slows down, but rpHSC numbers still need more than 12 months to get back to steady state levels—more time than the expected lifespan of a mouse at that age. In contrast, both mtHSC and progenitor numbers are predicted to show a similar behavior compared with the situation of a young mouse.

Upon downstream depletion, both mtHSC and progenitor recovery starts with rpHSC numbers being in steady state (Fig. 4B). Similar to the young situation, both mtHSC and progenitor levels are reached within few days due to logistic growth of the respective compartments. However, the combination of elevated demand of mtHSCs and the loss in asymmetric divisional capability of rpHSCs leads to a more pronounced increase of rpHSC numbers shortly after perturbation compared with the young situation. This results from a compensation effect in which the rpHSC compartment needs to balance the loss of its capability to differentiate by asymmetric division. Consequently, rpHSC numbers only slowly get back to steady state levels in the long run due to low background differentiation.

For the scenario, in which only rpHSCs are depleted (Fig. 4C), rpHSC numbers show a slight long-term increase but overall remain as low as in the young setting since proliferation is not considerably enhanced by mtHSC demand. Consequently, mtHSC and progenitor cell numbers remain almost unchanged upon rpHSC depletion and homeostatic hematopoiesis is almost exclusively maintained by mtHSCs.

In summary, the model predicts that an aged hematopoietic system reacts robustly to major challenges and preserves the general dynamics observed for the young situations in Figure 2 with a tendency of enhanced expansion of rpHSCs. These findings are in qualitative agreement with several experimental studies on transplantation of aged mice, which report multiclonal system repopulation on similar time scales compared with young recipients [60–62]. However, we wish to point out that those irradiation-based assays are not fully comparable to our simplifying model assumption, which does not recapitulate the effect of a damaged hematopoietic microenvironment.

Discussion

Regulation of hematopoiesis has been subject to intensive scientific debate for several decades [1, 3, 5–9, 11, 12, 63, 64]. It has become clear that even HSCs, that are residing on top of the hematopoietic differentiation hierarchy, are not homogeneous and present with an intrinsic level of heterogeneity. Increasingly refined identification protocols and label retaining assays have identified HSC subsets with increased long-term repopulating behavior in transplantation settings. However, recent findings on steady state hematopoiesis promote the concept that these HSC subsets are largely dispensable for supporting hematopoiesis under homeostatic conditions.

With our mathematical modeling approach, we show that these different phenomena can be embedded in a quantitative concept in which two HSC subsets respond differentially to varying demands. The most prominent feature of our approach is to define HSC turnover not as a direct function of the most primitive HSC population itself, but to attribute it to the on-demand regulation of a second, downstream HSC compartment. This approach does not exclude additional feedback loops from progenitor and peripheral blood compartments (as pursued in other works, for example [65, 66]), but demonstrates that HSC heterogeneity is a potential mechanism to explain the limited recovery of highly potent rpHSCs to targeted depletion of certain hematopoietic cell types [8]. Although our assumption might oversimplify a more complex regulation, our approach emphasizes a regulatory control mechanism below the rpHSC compartment that links continuous hematopoietic output with a rare activation of the rpHSC reservoir and is in agreement with a set of recent experimental findings [5, 6, 11]. In fact, coupling rpHSC turnover to the demand of mtHSCs is sufficient to explain a diverse set of phenomena. Our results confirm the observation that rpHSCs respond to a loss of more differentiated cell types with an increase in proliferation activity. Whenever downstream compartments have reached their respective steady state cell numbers, our modeling approach predicts decreasing proliferation of rpHSCs irrespective of their cell number. Consequently, a sole depletion of rpHSCs is not rapidly compensated, since no further demand is exerted from the downstream cell types. Hence, our model suggests that there is no or only a limited intrinsic regulation of the number of rpHSCs solely based on their own abundance. Furthermore, there is evidence for a loose regulation of the HSC compartment size from experiments with artificially increased HSC numbers which demonstrated their long-term engraftment, function, and maintenance [67].

We also demonstrate that a strong increase in rpHSC numbers is most likely induced by the substantially impaired ability of mtHSCs to retain their own population. This suggests that the proliferative ability of this mtHSCs population is more severely affected in irradiation settings as compared with targeted stem and progenitor depletion, that leaves the local microenvironment largely intact. A similar influence of the microenvironment on HSC recovery has recently been suggested in an elegant modeling approach by [68], which, unlike our approach, still expects a recovery of primitive HSC numbers after approximately 1 year. Based on our modeling results, we conclude that rpHSCs represent a rather autarkic cell population that only kicks in in case of strong demands that cannot be served by the mtHSCs themselves. Such demands may result either acutely from severe condition regimens or from progressive proliferative exhaustion on the long run.

We further extended our model approach to account for changes in polarity and divisional asymmetry during hematopoietic aging. Based on our observation, that the polarity of Cdc42 and of correlated histone marks as well as the ability to divide asymmetrically are markedly reduced in rpHSCs derived from older animals, we tested the hypothesis of an age-depended shift in the cells' ability to divide asymmetrically as a critical feature explaining the rpHSC pool expansion with aging. In contrast to the models presented in [65, 69, 70], we explicitly neglected symmetric differentiation of rpHSCs, since we did not observe such divisions in our biological experiments. The results of our ODE model reproduced the aging-related increase of rpHSC cell numbers, whereas mtHSC and progenitor numbers remained constant over time. Moreover, we were able to also quantitatively describe changes in the respective compartment size ratios. Taken together, our model supports the hypothesis that the aging-related shift from asymmetric to symmetric self-renewing rpHSC divisions is sufficient to describe phenomena of the aging rpHSC compartment. Since there is a correlation between the loss of polarity (with respect to Cdc42 and correlated histone marks) in rpHSCs and increasing numbers of symmetric divisions, our model emphasizes the idea that the shift from polar to apolar rpHSCs is a major driver of HSC aging. However, within the scope of this study, we did not consider any further aging-related distortions that might affect the cells' differentiation ability and potentially account for myeloid lineage bias or HSC exhaustion.

In contrast to previous modeling approaches of the HSC system by others [6, 66, 71–74] and us [54, 75], we here shift the focus from a self-sustaining and self-regulated rpHSC population toward a population that is dynamically regulated by downstream compartments while keeping the number of model parameters at a minimum. Other than in the demand-driven model proposed in [65], we place the focus on only rpHSC proliferation being driven by mtHSC demand rather than the most downstream compartment. Similarly, older model approaches discuss the role of asymmetric cell divisions in the context of balancing self-renewal and differentiation [4]. In contrast to these works, we study the role of an impaired maintenance of divisional asymmetry during aging as functional/epigenetic mechanism to account for the increase in rpHSCs.

The generalizability of our model approach (as of any other) is on the one hand limited by the simplifications which are necessary to acquire identifiable model solutions, whereas on the other hand restrictions apply for the available data. As an example, one could argue that also different progenitor stages are sequentially involved in the underlying regulation of rpHSCs or that there is an additional functional impairment of aged rpHSCs. However, without obtaining further data that investigates the system response to targeted, cell type specific perturbations, it is not possible to derive a more detailed understanding of further feedback regulations. As such, our focus is currently limited to the interplay between rpHSCs and mtHSCs, while the implemented progenitor compartment is directly coupled to the mtHSCs without further regulation.

Although our model approach adheres to the simplifying idea of reflecting different stages of HSC differentiation by the sequential coupling of intrinsically homogenous "compartments," we understand this concept as a simplification of an inherently continuous process (see also [64] and references therein). In the experimental context, the phenotypic definition of cell types is a powerful tool to prospectively identify populations that are enriched for certain functional potentials and to allow setting up comparable experimental protocols. However, the objection that transits between the different cell stages are most likely not instantaneous but gradual also applies to the model context. Here, the formulation in terms of disjunctive, intrinsically homogenous cell compartments owes to the simpler mathematical formalisms and the easier comparison to experimental data.

Conclusion

Our approach illustrates that mathematical models are an essential tool to not only conceptually but also quantitatively embed a range of diverse biological phenomena in a unifying context. We demonstrate this potential by applying a novel model of HSC

regulation to a range of observations in homeostatic situations that have challenged the prevailing view of an "almighty" stem cell. We conclude that a dynamically regulated and demand-driven approach is well-suited to explain hematopoiesis in the context of steady state blood production and response to stress and transplantation.

Acknowledgments

We thank Thomas Höfer for providing published time course data from [6]. This work was supported by an Emmy Noether Grant to M.C.F., by the German Research Council (DFG GE 3038/1-1) to A.G., and by the German Federal Ministry of Research and Education (BMBF, grant number 031A315 "MessAge") to I.G. and M.K.

Author Contributions

M.K., I.G.: conceived the mathematical model, wrote the final manuscript, final approval of manuscript; M.C.F., A.G., H.G.: designed and performed the experiments, contributed to discussions of the manuscript, final approval of manuscript.

Disclosure of Potential Conflicts of Interest

The authors indicated no potential conflicts of interest.

Data Availability Statement

Primary experimental data and simulation source code can be obtained from the authors upon request.

References

1 Moore KA, Lemischka IR. Stem cells and their niches. Science 2006;311:1880–1885.
2 Wilson A, Laurenti E, Oser G et al. Hematopoietic stem cells reversibly switch from dormancy to self-renewal during homeostasis and repair. Cell 2008;135:1118–1129.
3 Morrison SJ, Weissman IL. The long-term repopulating subset of hematopoietic stem cells is deterministic and isolatable by phenotype. Immunity 1994;1:661–673.
4 Wichmann HE, Loeffler M. Mathematical Modeling of Cell Proliferation: Stem Cell Regulation in Hemopoiesis, Vol. 1. Boca Raton, FL: CRC Press, Inc., 1985.
5 Chapple RH, Tseng YJ, Hu T et al. Lineage tracing of murine adult hematopoietic stem cells reveals active contribution to steady-state hematopoiesis. Blood Adv 2018;2:1220–1228.
6 Busch K, Klapproth K, Barile M et al. Fundamental properties of unperturbed haematopoiesis from stem cells in vivo. Nature 2015;518:542–546.
7 Rodriguez-Fraticelli AE, Wolock SL, Weinreb CS et al. Clonal analysis of lineage fate in native haematopoiesis. Nature 2018;553:212–216.
8 Schoedel KB, Morcos MNF, Zerjatke T et al. The bulk of the hematopoietic stem cell population is dispensable for murine steady-state and stress hematopoiesis. Blood 2016;128:2285–2296.
9 Sun J, Ramos A, Chapman B et al. Clonal dynamics of native haematopoiesis. Nature 2014;514:322–327.
10 Yu VW, Yusuf RZ, Oki T et al. Epigenetic memory underlies cell-autonomous heterogeneous behavior of hematopoietic stem cells. Cell 2016;167:1310.e17–1322.e17.
11 Sawai CM, Babovic S, Upadhaya S et al. Hematopoietic stem cells are the major source of multilineage hematopoiesis in adult animals. Immunity 2016;45:597–609.
12 Upadhaya S, Sawai CM, Papalexi E et al. Kinetics of adult hematopoietic stem cell differentiation in vivo. J Exp Med 2018;215:2815–2832.
13 Sawen P, Eldeeb M, Erlandsson E et al. Murine HSCs contribute actively to native hematopoiesis but with reduced differentiation capacity upon aging. eLife 2018;7:e41258.
14 Ganuza M, Hall T, Finkelstein D et al. Lifelong haematopoiesis is established by hundreds of precursors throughout mammalian ontogeny. Nat Cell Biol 2017;19:1153–1163.
15 Pei W, Feyerabend TB, Rossler J et al. Polylox barcoding reveals haematopoietic stem cell fates realized in vivo. Nature 2017;548:456–460.
16 Crisan M, Dzierzak E. The many faces of hematopoietic stem cell heterogeneity. Development 2016;143:4571–4581.
17 Muller-Sieburg CE, Sieburg HB, Bernitz JM et al. Stem cell heterogeneity: Implications for aging and regenerative medicine. Blood 2012;119:3900–3907.
18 Sieburg HB, Cho RH, Dykstra B et al. The hematopoietic stem compartment consists of a limited number of discrete stem cell subsets. Blood 2006;107:2311–2316.
19 Dykstra B, Kent D, Bowie M et al. Long-term propagation of distinct hematopoietic differentiation programs in vivo. Cell Stem Cell 2007;1:218–229.
20 Bernitz JM, Kim HS, MacArthur B et al. Hematopoietic stem cells count and remember self-renewal divisions. Cell 2016;167:1296.e10–1309.e10.
21 Sawen P, Lang S, Mandal P et al. Mitotic history reveals distinct stem cell populations and their contributions to hematopoiesis. Cell Rep 2016;14:2809–2818.
22 van der Wath RC, Wilson A, Laurenti E et al. Estimating dormant and active hematopoietic stem cell kinetics through extensive modeling of bromodeoxyuridine label-retaining cell dynamics. PLoS One 2009;4:e6972.
23 Qiu J, Papatsenko D, Niu X et al. Divisional history and hematopoietic stem cell function during homeostasis. Stem Cell Rep 2014;2:473–490.
24 Foudi A, Hochedlinger K, Van Buren D et al. Analysis of histone 2B-GFP retention reveals slowly cycling hematopoietic stem cells. Nat Biotechnol 2009;27:84–90.
25 Asada N, Takeishi S, Frenette PS. Complexity of bone marrow hematopoietic stem cell niche. Int J Hematol 2017;106:45–54.
26 Crane GM, Jeffery E, Morrison SJ. Adult haematopoietic stem cell niches. Nat Rev Immunol 2017;17:573–590.
27 Acar M, Kocherlakota KS, Murphy MM et al. Deep imaging of bone marrow shows non-dividing stem cells are mainly perisinusoidal. Nature 2015;526:126–130.
28 Morrison SJ, Scadden DT. The bone marrow niche for haematopoietic stem cells. Nature 2014;505:327–334.
29 Grinenko T, Arndt K, Portz M et al. Clonal expansion capacity defines two consecutive developmental stages of long-term hematopoietic stem cells. J Exp Med 2014;211:209–215.
30 Lauridsen FKB, Jensen TL, Rapin N et al. Differences in cell cycle status underlie transcriptional heterogeneity in the HSC compartment. Cell Rep 2018;24:766–780.
31 Cabezas-Wallscheid N, Buettner F, Sommerkamp P et al. Vitamin A-retinoic acid signaling regulates hematopoietic stem cell dormancy. Cell 2017;169:807.e19–823.e19.
32 Dykstra B, Olthof S, Schreuder J et al. Clonal analysis reveals multiple functional defects of aged murine hematopoietic stem cells. J Exp Med 2011;208:2691–2703.
33 Geiger H, de Haan G, Florian MC. The ageing haematopoietic stem cell compartment. Nat Rev Immunol 2013;13:376–389.
34 Rossi DJ, Bryder D, Zahn JM et al. Cell intrinsic alterations underlie hematopoietic stem cell aging. Proc Natl Acad Sci USA 2005;102:9194–9199.
35 Beerman I, Bhattacharya D, Zandi S et al. Functionally distinct hematopoietic stem cells modulate hematopoietic lineage potential during aging by a mechanism of clonal expansion. Proc Natl Acad Sci USA 2010;107:5465–5470.
36 Florian MC, Dorr K, Niebel A et al. Cdc42 activity regulates hematopoietic stem cell aging and rejuvenation. Cell Stem Cell 2012;10:520–530.
37 Henry CJ, Marusyk A, DeGregori J. Aging-associated changes in hematopoiesis and leukemogenesis: What's the connection? Aging 2011;3:643–656.
38 de Haan G, Van Zant G. Dynamic changes in mouse hematopoietic stem cell numbers during aging. Blood 1999;93:3294–3301.
39 Chambers SM, Shaw CA, Gatza C et al. Aging hematopoietic stem cells decline in function and exhibit epigenetic dysregulation. PLoS Biol 2007;5:e201.

40 Morrison SJ, Wandycz AM, Akashi K et al. The aging of hematopoietic stem cells. Nat Med 1996;2:1011–1016.
41 Sudo K, Ema H, Morita Y et al. Age-associated characteristics of murine hematopoietic stem cells. J Exp Med 2000;192:1273–1280.
42 Noda S, Ichikawa H, Miyoshi H. Hematopoietic stem cell aging is associated with functional decline and delayed cell cycle progression. Biochem Biophys Res Commun 2009;383:210–215.
43 Harrison DE. Long-term erythropoietic repopulating ability of old, young, and fetal stem cells. J Exp Med 1983;157:1496–1504.
44 Harrison DE, Astle CM, Stone M. Numbers and functions of transplantable primitive immunohematopoietic stem cells. Effects of age. J Immunol 1989;142:3833–3840.
45 Geiger H, Denkinger M, Schirmbeck R. Hematopoietic stem cell aging. Curr Opin Immunol 2014;29:86–92.
46 Rossi DJ, Bryder D, Seita J et al. Deficiencies in DNA damage repair limit the function of haematopoietic stem cells with age. Nature 2007;447:725–729.
47 Armanios M, Alder JK, Parry EM et al. Short telomeres are sufficient to cause the degenerative defects associated with aging. Am J Hum Genet 2009;85:823–832.
48 Ho TT, Warr MR, Adelman ER et al. Autophagy maintains the metabolism and function of young and old stem cells. Nature 2017;543:205–210.
49 Flach J, Bakker ST, Mohrin M et al. Replication stress is a potent driver of functional decline in ageing haematopoietic stem cells. Nature 2014;512:198–202.
50 Grigoryan A, Guidi N, Senger K et al. LaminA/C regulates epigenetic and chromatin architecture changes upon aging of hematopoietic stem cells. Genome Biol 2018;19:189.
51 Beerman I, Bock C, Garrison BS et al. Proliferation-dependent alterations of the DNA methylation landscape underlie hematopoietic stem cell aging. Cell Stem Cell 2013;12:413–425.
52 Sun D, Luo M, Jeong M et al. Epigenomic profiling of young and aged HSCs reveals concerted changes during aging that reinforce self-renewal. Cell Stem Cell 2014;14:673–688.
53 Florian MC, Klose M, Sacma M et al. Aging alters the epigenetic asymmetry of HSC division. PLoS Biol 2018;16:e2003389.
54 Glauche I, Moore K, Thielecke L et al. Stem cell proliferation and quiescence—Two sides of the same coin. PLoS Comput Biol 2009;5:e1000447.
55 Sheikh BN, Yang Y, Schreuder J et al. MOZ (KAT6A) is essential for the maintenance of classically defined adult hematopoietic stem cells. Blood 2016;128:2307–2318.
56 Hofer T, Rodewald HR. Differentiation-based model of hematopoietic stem cell functions and lineage pathways. Blood 2018;132:1106–1113.
57 Osawa M, Hanada K, Hamada H et al. Long-term lymphohematopoietic reconstitution by a single CD34-low/negative hematopoietic stem cell. Science 1996;273:242–245.
58 Essers MA, Offner S, Blanco-Bose WE et al. IFNalpha activates dormant haematopoietic stem cells in vivo. Nature 2009;458:904–908.
59 Wilson A, Laurenti E, Trumpp A. Balancing dormant and self-renewing hematopoietic stem cells. Curr Opin Genet Dev 2009;19:461–468.
60 Guidi N, Sacma M, Standker L et al. Osteopontin attenuates aging-associated phenotypes of hematopoietic stem cells. EMBO J 2017;36:840–853.
61 Ergen AV, Boles NC, Goodell MA. Rantes/Ccl5 influences hematopoietic stem cell subtypes and causes myeloid skewing. Blood 2012;119:2500–2509.
62 Liang Y, Van Zant G, Szilvassy SJ. Effects of aging on the homing and engraftment of murine hematopoietic stem and progenitor cells. Blood 2005;106:1479–1487.
63 Weissman IL. Stem cells: Units of development, units of regeneration, and units in evolution. Cell 2000;100:157–168.
64 Laurenti E, Gottgens B. From haematopoietic stem cells to complex differentiation landscapes. Nature 2018;553:418–426.
65 Marciniak-Czochra A, Stiehl T, Ho AD et al. Modeling of asymmetric cell division in hematopoietic stem cells—Regulation of self-renewal is essential for efficient repopulation. Stem Cells Dev 2009;18:377–385.
66 Manesso E, Teles J, Bryder D et al. Dynamical modelling of haematopoiesis: An integrated view over the system in homeostasis and under perturbation. J R Soc Interface 2013;10:20120817.
67 Shimoto M, Sugiyama T, Nagasawa T. Numerous niches for hematopoietic stem cells remain empty during homeostasis. Blood 2017;129:2124–2131.
68 Becker NB, Gunther M, Li C et al. Stem cell homeostasis by integral feedback through the niche. J Theor Biol 2018.
69 Loeffler M, Wichmann HE. A comprehensive mathematical model of stem cell proliferation which reproduces most of the published experimental results. Cell Tissue Kinet 1980;13:543–561.
70 Lander AD, Gokoffski KK, Wan FY et al. Cell lineages and the logic of proliferative control. PLoS Biol 2009;7:e15.
71 Abkowitz JL, Golinelli D, Harrison DE et al. In vivo kinetics of murine hemopoietic stem cells. Blood 2000;96:3399–3405.
72 Roeder I, Loeffler M, Quesenberry PJ et al. Quantitative tissue stem cell modeling. Blood 2003;102:1143–1144. author reply 1144–1145.
73 Engel C, Scholz M, Loeffler M. A computational model of human granulopoiesis to simulate the hematotoxic effects of multicycle polychemotherapy. Blood 2004;104:2323–2331.
74 Maloy M, Maloy F, Jakobsen P et al. Dynamic self-organisation of haematopoiesis and (a)symmetric cell division. J Theor Biol 2017;414:147–164.
75 Glauche I, Thielecke L, Roeder I. Cellular aging leads to functional heterogeneity of hematopoietic stem cells: A modeling perspective. Aging Cell 2011;10:457–465.

See www.StemCells.com for supporting information available online.